ISSN: 0975-8585

Research Journal of Pharmaceutical, Biological and Chemical Sciences

Revisiting Biological and Biomechanical Compatibility of Surgical Stents.

Vladimir Fedorovich Kulikovskyi*, Sergey Valentinovich Shkodkin, Yuri Romanovich Kolobov, Georgyi Viktorovich Chramov, Oleg Vladimirovich Miroshnichenko, and Alexei Vasilevich Lyubushkin.

Federal State Autonomous Educational Institution of Higher Professional Education, Belgorod State National Research University, 85, Pobedy St., Belgorod, 308015, Russia.

ABSTRACT

The article investigates hardness of a spiral of a nanotructural spiral stent. The stent biological and biomechanical compatibility was examined in the course of drainage of the native gullet of rats. The degree of microcirculation disorders and inflammatory changes in the gullet wall depended on hardness of the stent spiral.

Keywords: medical implant, stent, inflammation, drainage, biological compatibility, biomechanical compatibility.

Corresponding author

ISSN: 0975-8585

INTRODUCTION

Relevancy of internal stents use in surgery of pancreatobiliary region and the renal duct is practically assured due to minimum injuries and comparative manipulatory simplicity and at the present time their use is being regarded as the most preferable method of drainage [1 – 4]. Presence of a stent in a hollow organ lumen is accompanied by microcirculatory and inflammatory changes of its wall and the stent obstruction [5,6]. Such situation in this sphere results in high scientific interest aimed at medical stents improvement [7]. The major part of investigations resolves the problem of the surface quality improvement by introduction of hydrophilic coatings, impregnation with drug substances etc. [2, 8-10].

METHODOLOGY

Investigation of biological and biomechanical compatibility of the experimental nanostructural spiral stent (NSS) as well as of possibility of its removal through a hollow organ wall was performed in the course of its implantation in the gullet of 40 rats.

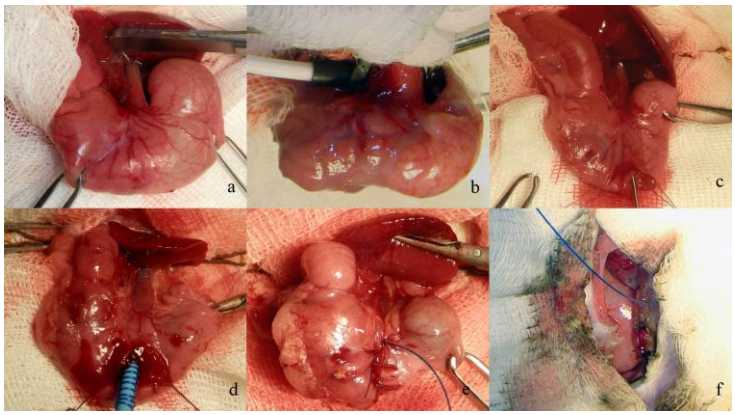

Figure 1: Implantation of experimental NSS in the gullet of a rat

In the control panel 20 animals were subject to implantation of a spiral stent 8 Ch with the length of 4 cm made of wire with the diameter of 0.25 mm from titanium alloy with the shape memory effect based on Ti-Ni-(X). The rest half of the animals (which were included into the basic panel) was subject to implantation of a spiral stent with identical external geometric parameters having a non-spiral part and made of prolene wire with the diameter of USP 2 (0.6 mm), the stent had protective original nanostructural coating based on amorphous carbon and silver nanoparticles (Fig. 1d). In order to prevent migration the distal stent ends were fixed by an interrupted endostitch polysorb 5-0 going through all layers of the wall (Fig. 1e). The non-spiral part was led out through the stomach wall (Fig. 1e), the muscles of the front abdominal wall (Fig. 1f) and 2 cm of the free end were implanted subcutaneously. The animals were drawn out the experiment on the 14^{th} and the 30^{th} day. On the mentioned dates examination of morphological changes in the gullet wall was performed.

MAIN PART

The elastic coefficient of the stent spiral made of titanium alloy with the shape memory effect based on Ti-Ni-(X) after testing of ten samples made 635.6±23.1 N/m, the spiral of prolene wire had the elastic coefficient of 58.4±7.3 N/m. No fatal cases were observed in the course of biological and biomechanical compatibility investigation of the experimental NSS at time of implantation in the rats' gullets. Five animals died in the control panel on the 13^{th}, 16^{th} (two of them), 17^{th} and 19^{th} day which made 25%. The section revealed purulent mediastinitis due to the gullet perforation in the zone of the proximal stent end.

By the 14^{th} day of a post-surgical period the morphological examination of the gullet in the control panel detected apparent hypertrophical and inflammatory changes in all of its wall layers. The latter were located predominantly near the proximal stent end and the stomach cardiac sphincter. Inflammatory infiltration involved all layers of the gullet wall. Leukocytic infiltrations consisted mainly of polymorphonucleocytes with acidophilic cytoplasm: 286±51 cells per HPF. Content of small lymphocytes and histiocytes in the infiltrations did not exceed 41±20 cells per HPF and 27±11 cells per HPF correspondingly. The

fascia bounding the adventitious layer could not be differentiated due to intense infiltration, the infiltrations thickness made 897.4±171.6 µm (Fig. 2a). Changes on the part of the mucous membrane included dystrophy, hypertrophy with increase of the number of layers of multilayer squamous epithelium up to 9-11 and formation of pseudopolyps, the mucous membrane thickness reached 142.5±20.9 µm. The mucous membrane surface was demonstrating extensive adhesion of bacterial population accompanied by invasion into its depth which was likely to cause inflammatory changes in the gullet wall and the fatal cases in the control panel. The bacterial cells in the amount of 165±48 cells per HPF proliferated up to the level of malpighinan layer and the mucous membrane basilemma with obvious edema of the submucosal layer as deep as 251.7±54.9 µm. The muscular layer hypertrophy was more distinctly differentiated beyond the inflammatory changes zone, the myocytes dystrophy phenomenon accompanied leukocytic infiltration, the muscular layer thickness made 1128.4±115.1 µm (Fig. 2b).

During the mentioned observation time examination of the basic panel revealed insignificant inflammatory changes which were presented by diffusely located (predominantly in adventitia and in the submucous layer) small lymphocytes in the amount of 37±12 cells per HPF and histiocytes – 12± cells per HPF ($p<0.01$, Fig. 2d). Polymorphonucleocytes with acidophilic cytoplasm were sporadic and were located in the mediastinal tissue ($p<0.01$). The mucous membrane included 3-5 layers of multilayer squamous epithelium cells, its thickness made 45.1±14.4 µm ($p<0.01$). Bacterial colonization of the horny layer is less intense, bacterial cells (37±11 cells per HPF) didn't reach the spinous layer ($p<0.01$). A moderate edema of the submucous layer was positively lower then that of the control panel – 77.1±24.9 µm ($p<0.05$). Hypertrophy and dystrophic changes in the muscular layer were not observed, the muscular layer thickness did not exceed 481.3±73.7 µm ($p<0.01$). The adventitia did not contain focal leucocytic infiltration, its thickness made 90.5±10.1 µm ($p<0.01$, Fig. 2c).

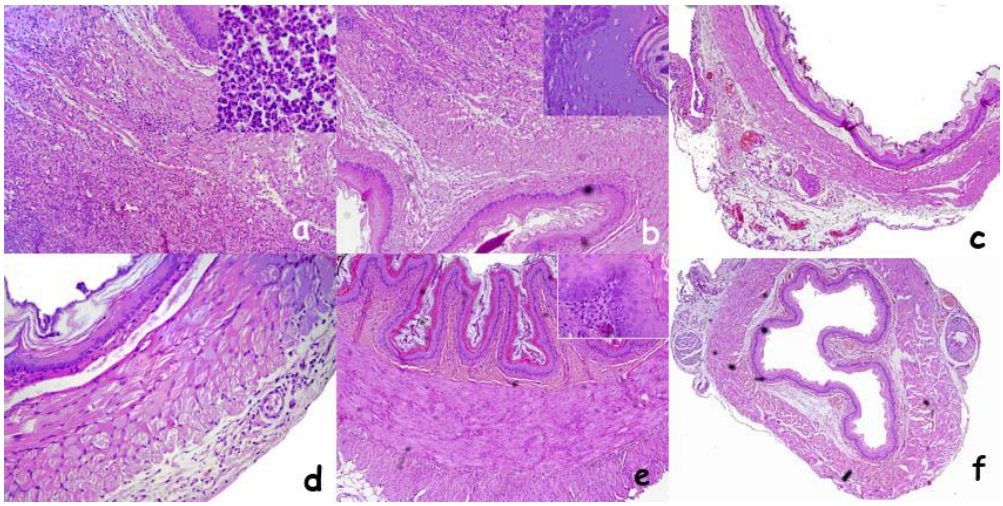

Figure 2: Cross section of the gullet wall at the level of the stent introduction. Stained with hematoxylin and eosin.
a –Microphoto. X 100 (X400); b – Microphoto. X 100 (X400); c – Microphoto. X 100; d – Microphoto. X 200; e – Microphoto. X 100 (X400); f – Microphoto. X 50.

On the 30th day of observation the microscopic presentation of the gullet of the survived animals in the control panel was characterized by reduction of intensity of the inflammatory cell response, of edema and consequently the gullet wall thickness as well as by development of sclerotic changes with the maximum prevalence in the submucous layer, at that the thickness of the latter didn't positively change as compared to the previous time interval and constituted 186.1±43.6 µm ($p>0.05$). The mucous membrane continued to demonstrate pseudopolyposis, dystrophyc changes with vacuolation of the malpighian layer cells cytoplasma and growth of number of the cell sheet layers up to 7-8, at that the mucous membrane showed week thickness decrease as compared to the 14th day of observation in this panel: up to 118.5±9.8 µm ($p>0,05$). There were bacterial agglomerations between the pseudopolyps, bacterial invasion at a depth of the mucous membrane spinous layer was registered (up to 93±26 cells per HPF), which is positively lower then in the previous time interval ($p<0,05$). The muscular layer demonstrated the maximum inflammatory infiltration reduction which was accompanied by positive decrease of the layer thickness to the value of 793.7±72.3 µm ($p<0.05$, (Fig. 2e).

Leukocytic infiltrates are of combined type and are represented by fine-focal aggregates of diffusely located lymphocytes (Fig. 8d). The leukocytic infiltration maximum intensity was registered in the submucous layer and the adventitia (Fig. 8e, f), the adventitia thickness made 506.5±77.2 µm. Large-focal and diffuse infiltrates like before predominantly contained polymorphonucleocytes with acidophilic cytoplasm (124±37 cells per HPF). A share of small lymphocytes – 89±23 cells per HPF as well as of histiocytes – 44±19 cells per HPF increased. Fibroblastic response was represented by cellular tissue fibers, fibrocytes – 55±16 cells per HPF and fibroblasts – 51±22 cells per HPF (Fig. 2e).

To the contrary the basic panel at this time interval demonstrated some progression of inflammatory changes due to the stent presence which like on the 14th day was positively lower then that in the control panel and was limited by the mucous and submucous layers. The mentioned layers had the following thickness: 57.1±6,2 and 115.3±31.2 µm correspondingly ($p<0.05$c). Changes in the submucous layer consisted in accumulation of cellular tissue by means of functional activity increase of fibrocytes – 28±9 cells per HPF as well as of fibroblasts – 15±9 cells per HPF ($p<0.05$). Leucocytic infiltration was mainly represented by the agranulocytic cells: small leukocytes – 54±17 cells per HPF and histiocytes – 29±14 cells per HPF ($p<0.01$), polymorphonucleocytes were sporadic. These changes in the mucous membrane and, predominantly, in the submucous layer became a reason for pseudopolyps formation. Hypertrophic and dystrophic changes in the mucous membrane were less intense then in the control panel, the number of layers in the mucous membrane reached 4-6 layers, bacterial invasion like in the previous interval didn't permeate deeper then the spinous layer and made – 33±14 cells per HPF ($p<0,01$). Like on the 14th day of investigation inflammatory infiltration and hypertrophic changes in the muscular layer were absent, its thickness which made 389.9±41.3 µm ($p<0,05$) was positively lower then that in the control panel and showed no difference with the previous time period. Leukocytic infiltration in the adventition was not intense and was represented by diffusely located agranulocytes (Fig. 2f).

FINDINGS

The both stents demonstrated adequate drainage function by ensuring the gullet patency within one month. Low indices of biomechanical compatibility of the stent in the control panel are evidenced by hypertrophic changes in the gullet muscular layer (by 2.1 – 2.3 times as compared to the basic panel). Use of bioinert coating based on amorphous carbon and silver nanoparticles and higher indices of biomechanical compatibility of the stent spiral (by 5.8 times) resulted in reduction of inflammatory leucocytic infiltration intensity which eliminated the gullet perforations and fatal cases in the basic study panel.

CONCLUSION

- Lesser spiral hardness of the experimental NSS reduced incidence of microcirculatory disorders as compared to the control panel.
- Better indices of NCC biomechanical compatibility prevented hypertrophic changes in the gullet wall, inflammatory infiltration and excluded fatal cases in the basic panel.

REFERENCES

[1] Barut, I. and O.R. Tarhan, 2014. Cecum perforation due to biliary stent migration. Saudi Med J., Jul;35(7):747-9.

[2] Shkodkin, S.V., M.I. Kogan, Y.B. Idashkin et al., 2012. Comparative analysis of utilization efficiency of polyurethane and nanostructural stents at time of experimental upper urinary tracts drainage. Vestnik transplantologii I iskusstvennykh organov, 14(4): 65-73.

[3] Boeckel, P.G., F.P. Vleggaar and P.D. Siersema, 2009. Plastic or metal stents for benign extrahepatic biliary strictures: a systematic review. BMC Gastroenterol., Dec 17;9:96.

[4] Burks, F.N. and R.A. Santucci, 2014. Management of iatrogenic ureteral injury. Ther Adv Urol., Jun;6(3):115-124.

[5] Choong, H.R. and K.L. Sung, 2011. Biliary Strictures after Liver Transplantation. Gut Liver., Jun; 5(2): 133–142.

[6] Ito, K., T. Ogawa, J. Horaguchi et al., 2013. Reintervention for occluded biliary metal stent for patients with malignant distal biliary stricture. Dig Endosc., May;25 Suppl 2:126-31.

[7] Lee, P., E. Kupeli and A.C. Mehta, 2010. Airway stents. Clin Chest Med., Mar;31(1):141-50.

[8] Liatsikos, E., P. Kallidonis, J.U. Stolzenburg and D. Karnabatidis, 2009. Ureteral stents: Past, present and future. Expert Rev Med Devices, 6:313–24.

[9] Shkodkin, S.V., S.V. Ivanov, Y.B. Idashkin et al., 2012. Experimental bioinertness investigation of materials used in production of surgical stents. Kursk scientifical and practical journal "Man and his health", 4: 32-39.

[10] Kolobov, Y.R., 2009. Technologies of structure and properties synthesis of titanium alloys for medical implants with bioactive coatings. Nanotechnologies in Russia, 4(11-12): 69-81.